

This discussion paper is/has been under review for the journal *Atmospheric Chemistry and Physics (ACP)*. Please refer to the corresponding final paper in *ACP* if available.

**Influence of  
entrainment of CCN**

J. W. B. Derksen et al.

# Influence of entrainment of CCN on microphysical properties of warm cumulus

J. W. B. Derksen, G.-J. H. Roelofs, and T. Röckmann

Institute for Marine and Atmospheric Research Utrecht, Utrecht, The Netherlands

Received: 3 February 2009 – Accepted: 24 March 2009 – Published: 2 April 2009

Correspondence to: J. W. B. Derksen (j.w.b.derksen@uu.nl)

Published by Copernicus Publications on behalf of the European Geosciences Union.

Title Page

Abstract

Introduction

Conclusions

References

Tables

Figures

◀

▶

◀

▶

Back

Close

Full Screen / Esc

Printer-friendly Version

Interactive Discussion



## Abstract

We use a 1-D cloud model with explicit microphysics and a binned representation of the aerosol size distribution to investigate the influence of entrainment of cloud condensation nuclei (CCN) on the microphysical development of warm cumulus clouds.

5 For a more realistic representation of cloud drop spectral width, the model separates droplets that grow on aerosol that is initially present in the cloud from droplets growing on entrained aerosol. Model results are compared with observations of trade wind cumulus microphysics from the Rain in Cumulus over the Ocean experiment (RICO, 2004–2005). The results indicate that CCN are entrained throughout the entire cloud  
10 depth, and inside the cloud part of these may be activated. Compared to a simulation where entrainment of ambient CCN is neglected this leads to higher cloud droplet number concentrations (CDNC) and a continuous presence of droplets in the range smaller than  $\sim 5 \mu\text{m}$  that is consistent with the observations. Cloud dynamics are sensitive to the entrainment parameter as well as to the applied initial vertical velocity, as  
15 expressed by the liquid water content and cloud top height. However, simulated cloud drop spectra remain relatively unaffected for the specific conditions during RICO.

## 1 Introduction

Anthropogenic emissions of primary aerosol particles and aerosol precursors (sulfur dioxide, non-methane higher hydrocarbons, nitrogen oxides, soot) have increased atmospheric aerosol concentrations substantially since pre-industrial times (e.g., Charlson et al., 1992; Solomon et al., 2007). Aerosols act as cloud condensation nuclei, and the increasing aerosol abundance and changing chemical composition affect climate through the so-called aerosol indirect effects. In the first indirect effect, an increase of aerosol particles leads to a higher cloud droplet number concentration, a smaller average drop radius and a larger optical thickness (Twomey, 1977). In the second indirect  
25 effect, the efficiency of precipitation formation decreases because of the smaller drop

## Influence of entrainment of CCN

J. W. B. Derksen et al.

Title Page

Abstract

Introduction

Conclusions

References

Tables

Figures

◀

▶

◀

▶

Back

Close

Full Screen / Esc

Printer-friendly Version

Interactive Discussion



size, and the cloud lifetime increases (Albrecht, 1989).

The cloud drop number concentration (CDNC) is a crucial parameter for both effects (Lohmann and Feichter, 2005). Since it is associated with the average droplet size it is relevant for cloud scattering as well as for drizzle formation. The initial CDNC is determined directly at the cloud base. Much research effort has been invested therefore in understanding how meteorological characteristics and aerosol properties influence aerosol activation at the cloud base (e.g., Kulmala et al., 1993), and in the development of parameterizations for CDNC that can be used in general circulation models (e.g., Hänel, 1987; Fountoukis and Nenes, 2005). In the second place, the distribution of the liquid water with droplet size further influences both scattering and precipitation formation processes (e.g., Roelofs and Jongen, 2004; Roelofs and Kamphuis, 2009). A model study of cloud microphysics therefore requires a realistic representation of both CDNC and the drop size distribution.

During adiabatic cloud development the liquid water content (LWC) evolves adiabatically with height and, when neglecting collision/coalescence between droplets, CDNC remains constant throughout the cloud depth (Pruppacher and Klett, 1978). However, many observed clouds develop in a sub-adiabatic manner, with continuous entrainment of surrounding subsaturated air into the cloud, resulting in smaller LWC and CDNC than their adiabatic values (e.g., Penner and Chuang, 1999; Gerber et al., 2005; Meskhidze et al., 2005). Simultaneously, the entrained air contains unactivated aerosol. During mixing with cloudy air these are exposed to supersaturation conditions and may partly activate. Thus, small and recently activated droplets are added continuously to the cloud air and this results in a broadening of the drop size distribution. The mixing process between the cloud air and the entrained air is thought of as being homogeneous or inhomogeneous (Su et al., 1998). In homogeneous mixing the typical time scale of the mixing, through turbulence, is small compared to the typical time scale for condensational growth of the entrained particles. In that case, the entrained drops and the drops initially present in the cloud are subjected to the same saturation. In inhomogeneous mixing, on the other hand, the mixing time scale is larger than the time scale for

**Influence of entrainment of CCN**

J. W. B. Derksen et al.

Title Page

Abstract

Introduction

Conclusions

References

Tables

Figures

◀

▶

◀

▶

Back

Close

Full Screen / Esc

Printer-friendly Version

Interactive Discussion



condensational growth, and different droplets encounter different saturation conditions. Both mixing processes have been observed (Paluch, 1986; Blyth and Latham, 1990; Hicks et al., 1990; Burnet and Brenguier, 2007).

The microphysical evolution of drops in an entraining cloud with inhomogeneous mixing can be represented adequately only in a 2-D or 3-D cloud resolving model with detailed representations of turbulent mixing and aerosol microphysics, but these are computationally expensive. In parcel model studies, where the cloud is represented as a homogeneous air mass, detailed microphysical calculations are more feasible (e.g., Kreidenweis et al., 2003). Mixing of entrained air in a cloud parcel model is always homogeneous. In order to preserve the information held by the simulated drop size distribution it is necessary, however, to separate the representations of larger, older cloud drops and smaller entrained particles. We remark that the value of the entrainment parameter is rather uncertain. Values ranging from  $0.1/R$  to  $0.6/R$ , with  $R$  the cloud parcel radius, are derived from observations and applied in different model studies (Su et al., 1998; Roesner et al., 1990; Pruppacher and Klett, 1978; Roelofs and Jongen, 2004).

In this model study we examine the influence of entrainment of relatively dry air containing aerosol on cloud dynamical and microphysical parameters. We use a one-dimensional (1-D) cloud column model that contains a binned representation of aerosol. It simulates aerosol activation, condensational growth and evaporation based on Köhler microphysics. The representation of the drop size distribution in the model enables a separate evaluation of entrained drops and mature cloud drops, as described in more detail in Sect. 2. The model is applied to the simulation of a typical trade cumulus cloud observed during RICO (Rain in Cumulus over the Ocean; Rauber et al., 2007). The measurement campaign was carried out during December 2004–January 2005 and was located near the islands of Antigua and Barbuda, an area under influence of persistent trade winds. Simulated vertical profiles of cloud water, CDNC, average cloud drop size and cloud drop size distribution are evaluated, and their sensitivity to dynamical parameters (entrainment efficiency, updraft velocity) is examined. Section 3

---

**Influence of  
entrainment of CCN**J. W. B. Derksen et al.

---

[Title Page](#)[Abstract](#)[Introduction](#)[Conclusions](#)[References](#)[Tables](#)[Figures](#)[◀](#)[▶](#)[◀](#)[▶](#)[Back](#)[Close](#)[Full Screen / Esc](#)[Printer-friendly Version](#)[Interactive Discussion](#)

describes the relevant observations from RICO. In Sect. 4 the results of the study are presented, and Sect. 5 presents a discussion of the results and the conclusions.

## 2 Model description

We use a one-dimensional circular axisymmetric cloud model (Ogura and Takahashi, 1971; Takahashi, 1976). We implemented the detailed microphysical module applied in the cloud parcel model by Roelofs and Jongen (2004). In addition, the model now incorporates a detailed representation of entrained cloud condensation nuclei (CCN) and their evolution. Ice formation and radiative transfer are not simulated.

The model simulates a vertical cloud column with a radius of 300 m. Around this column a passive circular concentric column is present, representing the cloud environment, where all properties are kept constant. The domain ranges from 0 to 4 km altitude with a vertical grid distance of 100 m and a time resolution of 0.1 s. Upper and lower boundaries are closed and associated quantities are kept constant.

Vertical motions of air are suppressed at the upper and lower boundaries and are controlled by buoyancy and drag in the interior. Exchange between the cloud and the environment occurs in two ways. In the first place, convergence and divergence in the computed vertical velocity field in the cloudy column drive in- and outflow through the lateral boundary. In the second place lateral mixing occurs. The strength of lateral entrainment is set through the fractional entrainment rate,  $|w|\frac{\alpha}{R}$ , where  $w$  is the vertical velocity,  $R$  is the radius of the cloud and  $\frac{\alpha}{R}$  is the entrainment parameter. The fractional entrainment rate determines the volume fraction of a model grid space which is exchanged with the environment every time step. In our study we use a value of 0.4 for  $\alpha$ , unless stated otherwise. This is consistent with Gerber et al. (2008) who showed that during RICO on the 11th of January (the data used in this study is observed on this date, see Sect. 3 for details) the average fractional entrainment,  $\frac{\alpha}{R}$ , for the lower 1.5 km is  $1.3\text{ km}^{-1}$  with an observed mean width of the towering cloud tops (i.e.,  $2R$ ) of 550 m. Lateral entrainment decreases gradients between cloudy and ambient air.

### Influence of entrainment of CCN

J. W. B. Derksen et al.

Title Page

Abstract

Introduction

Conclusions

References

Tables

Figures

◀

▶

◀

▶

Back

Close

Full Screen / Esc

Printer-friendly Version

Interactive Discussion



---

**Influence of  
entrainment of CCN**J. W. B. Derksen et al.

---

[Title Page](#)[Abstract](#)[Introduction](#)[Conclusions](#)[References](#)[Tables](#)[Figures](#)[I◀](#)[▶I](#)[◀](#)[▶](#)[Back](#)[Close](#)[Full Screen / Esc](#)[Printer-friendly Version](#)[Interactive Discussion](#)

Aerosols are represented by a discrete size distribution, that ranges from 0.002 to 5  $\mu\text{m}$  and is divided in 50 bins. Each size bin has a continuously modified wet radius associated with it, that is modified through condensation or evaporation. Aerosol activation and condensation/evaporation of water are calculated according to the Köhler equations, parameterized according to Hänel (1987). The collision-coalescence process is parameterized according to Jacobson (1998). Drops formed through collision-coalescence are transferred to a discrete size distribution with 50 bins, ranging from 0.1 to 2000  $\mu\text{m}$ . These droplets are also subject to condensation and evaporation. They may be removed from the cloud as rain due to their relatively large fall velocities.

During cloud development, ambient CCN are entrained into the cloud and a part becomes activated after mixing with the supersaturated cloud air. That implies that at any moment, besides older larger droplets, small droplets with a size of the order of several micrometers are present at any level within the cloud. To optimally represent both the droplets formed during the cloud onset and the droplets growing on entrained particles, their evolution has to be considered separately, i.e. in separate droplet size distributions. However, in order to keep the computational time limited the different distributions must be combined at specific instants during the simulation. The time interval between different averaging events,  $t_m$ , must reflect the time for condensational growth from their critical size to typical cloud drop sizes. This period of time depends on the supersaturation, i.e. the speed of condensational growth. During simulations the typical supersaturation is 0.4%. At this supersaturation, a droplet of 1  $\mu\text{m}$  needs 90 s to grow to a size of 8  $\mu\text{m}$  and 300 s to grow to 15  $\mu\text{m}$ .

In the present version, the model contains four different aerosol/drop size distributions. One distribution is assigned to represent the aerosol/droplets initially present in the column and another distribution represents the most recently entrained CCN. The remaining distributions represent previously entrained particles. In a sensitivity study, we obtained good results for  $t_m=100$  s. This means that every 100 s each distribution is shifted to the next, and 300 s after their entrainment, particles are combined with the distribution that carries the initial cloud aerosol.

### 3 RICO and data description

The Rain In Cumulus over the Ocean (RICO) field campaign took place during November 2004–January 2005 off the Caribbean Islands of Antigua and Barbuda. The area is characterized during this period by shallow trade wind cumuli, most frequently topping at 800 hPa under the influence of an inversion layer. Convection reaching up to 700 hPa and higher has been observed.

A goal of the campaign was to gain insight in the rain initiation processes within shallow maritime cumulus. Therefore, cloud properties such as LWC and droplet size distributions were measured. Also vertical temperature and humidity profiles were measured with dropsondes. CCN measurements were done during low altitude circles at 100 m height. Clouds were measured by the C130 aircraft at 5 different height levels (800, 1000, 1200, 1500 and 1650 m) at 1 Hz, corresponding to approximately 100 m flight distance. We focus on data measured on the 11th of January, which was characterized by lower drizzle concentrations than other RICO days (Gerber et al., 2008). For these circumstances, effects of entrainment can be studied without influence of LWC depletion by precipitation.

We applied two criteria to filter the data: 1) The measured LWC is larger than 0.05 g/kg and 2) the vertical velocity is positive. This excludes cloudless regions and in-cloud parts dominated by downdrafts and emphasizes the cloud cores simulated by our model. The resulting data set is an ensemble of many different clouds, in a different stage of development and measured at a different location, both geometrically as well as with respect to the position within a cloud.

To compare model results with observations, the same criteria are used to sample the model domain. For both simulated and observed data sets we calculated median values for LWC, mean radius ( $r_m$ ) and CDNC, as well as for the total size distributions. The observed and simulated data sets are different in that sense that the observations reflect an ensemble of “snap-shots” of many different clouds, whereas the model reflects one complete cloud evolution of an average cloud. We will investigate if the

Title Page

Abstract

Introduction

Conclusions

References

Tables

Figures

◀

▶

◀

▶

Back

Close

Full Screen / Esc

Printer-friendly Version

Interactive Discussion



modeled cloud does represent the average evolution of the RICO ensemble. We remark that the observed 1650 m level only consists of two data points.

## 4 Initialization and results

### 4.1 Model initialization

5 Sonde data from 14:40 UTC (see Fig. 1) were used to initialize the vertical temperature and specific humidity profiles in the model. The sounding reflects a dry adiabatic lapse rate ( $\sim -10$  K/km) from the surface up to 600 m height, the location of the lifting condensation level, and a lapse rate of  $-7$  K/km from 600 m to 1700 m, which is conditionally unstable. An inversion layer was located at 1700 m. Small scale vertical variations can  
10 not be represented due to the relative coarse model resolution. Hence, we used the observed lapse rates as input. Surface temperature is initialized at 298.5 K. We remark that the observed horizontal variability of relative humidity (RH) ranges up to ten percent, indicating a significant spatial variability of the atmospheric conditions under which the cumulus clouds are formed.

15 The average observed in-cloud vertical velocity at 800 m altitude, the approximate cloud base height, is 1.18 m/s. Generally, larger updraft velocities are associated with larger values for LWC. We assumed an initial vertical updraft velocity below the cloud base of 1.5 m/s and investigated the sensitivity of the simulated cloud characteristics for variations in the updraft velocity.

20 The aerosol size distribution is initialized based on daily averaged values of CCN measurements (see Hudson and Mishra (2007) for details). A three-modal lognormal distribution is fitted to the observations (see Table 1). Hudson and Mishra (2007) found that CCN concentrations showed little variability during each low altitude flight, though concentrations increased during the day. Gerber et al. (2008) found that the CCN concentration at 1.5% supersaturation was approximately constant with height, indicating  
25 a well mixed boundary layer. Therefore, we took an aerosol scaleheight of 8000 m,

Title Page

Abstract

Introduction

Conclusions

References

Tables

Figures

◀

▶

◀

▶

Back

Close

Full Screen / Esc

Printer-friendly Version

Interactive Discussion



resulting in a near constant CCN concentration throughout the boundary layer. Peter et al. (2008) showed that most aerosol larger than  $0.2\ \mu\text{m}$  consisted of sea salt, but that aerosol smaller than  $0.2\ \mu\text{m}$  consisted mostly of ammonium sulphate. For computational reasons we assume all aerosol to consist of sea salt. This assumption can lead to a slightly smaller cutoff radius and thus larger CDNC, but the differences are insignificant compared to the effect of spatial variabilities in humidity mentioned above. The environmental column is initialized with the same aerosol size distribution and vertical profile and assumed to be constant throughout a simulation.

## 4.2 Analysis of the base case

Figure 2 shows the simulated profiles of LWC and its sensitivity for humidity, of CDNC and of the median radius, together with the observations. It is stressed that the observed data ensemble at 1650 m altitude consists of two measurements. To avoid a misleading figure, the mean of the observations is shown at this height, since the median would be one of both measurements. The vertical profile of the simulated median LWC is qualitatively similar to the observed profile. The median increases from the cloud base up to  $\sim 1.2$  km altitude. Between 1200 and 1500 m altitude the model predicts a decrease. No observations are available at these heights to verify this result. Just below cloud top the simulated median value increases again in agreement with the observations. Similar LWC profiles were found in other trade wind cumulus studies (e.g., Lu et al., 2003). The LWC profile reflects the RH profile, with local maxima of  $\sim 90\%$  at 500 and 1500 m altitude (see Fig. 1). The cloud entrains increasingly moist air above 1200 m, leading to an increasing saturation level in the cloud which supports condensation of water vapor.

The model underestimates the median LWC throughout the cloud depth (up to 50% below the cloud top), as well as the range in observed LWC values. To investigate the sensitivity of LWC for humidity, we performed two additional simulations, with 99% and 101% of the original specific humidity respectively. The results are shown in Fig. 2b. At lower humidity, the simulated cloud already dissipates below 1400 m and 90% val-

Title Page

Abstract

Introduction

Conclusions

References

Tables

Figures

◀

▶

◀

▶

Back

Close

Full Screen / Esc

Printer-friendly Version

Interactive Discussion



ues remain below 0.3 g/kg throughout the cloud depth. A higher humidity does not result in an increase of the median LWC values, but the 90% values are raised from 0.34 to 0.4 g/kg. We conclude that varieties in humidity may partly account for the disagreement between observed and simulated range in the LWC, but do not explain the underestimation of the median values in the upper cloud areas by the model. We remark, however, that at altitudes just above cloud base the RICO data represent clouds characterized by a wide range of updraft velocities, whereas at higher altitudes only clouds with a more vigorous updraft are represented. The latter are characterized by relatively large LWC.

Simulated CDNC (Fig. 2c) is in the same order of magnitude as the observed CDNC. However, the model simulates a gradual decrease with height that is not observed. The aerosol scale height of 8000 m applied in our study only has a small influence on this. We suspect that the fact that the cloud ensemble represented in the RICO data is different for different altitudes, as mentioned above, also influences the observed CDNC profiles. The range towards small concentrations is very well captured by the model. Towards high concentrations, the model underestimates the range increasingly with height, up to 35% at 1500 m. Discrepancies between observed and simulated range in LWC and CDNC are probably associated, suggesting that more vigorous clouds, growing in more humid air and with relatively large CDNC caused by larger updraft velocities, have a relatively large weight within the observed data set.

The simulated median values of  $r_m$  shown in Fig. 2d, agree well with the observed median. An increase from 8 up to 11  $\mu\text{m}$  is simulated between 800 and 1000 m altitude, above which  $r_m$  is nearly constant up to 1500 m. In the cloud top,  $r_m$  increases again, up to 12  $\mu\text{m}$ , which is a slight underestimation compared to the observed increase up to 13  $\mu\text{m}$ . A good agreement is found with the profile compiled by Arabas et al. (2009). The 10% percentile in the model is far too low compared to the observations. Closer inspection reveals that only during a small fraction of the cloud evolution such small mean radii are simulated, whereas such values are rare in the observations. This suggests that these small mean radii are a property of clouds in a very early (the first

**Influence of  
entrainment of CCN**

J. W. B. Derksen et al.

Title Page

Abstract

Introduction

Conclusions

References

Tables

Figures

◀

▶

◀

▶

Back

Close

Full Screen / Esc

Printer-friendly Version

Interactive Discussion



minute) stage or in the last moments of dissipation and have a low probability to be measured by aircraft.

To assess the influence of entrainment of ambient CCN into the cloud, we performed a simulation without ambient CCN. Figure 3 shows the simulated profiles of LWC, CDNC and  $r_m$ .

Compared to the simulation with ambient CCN, i.e. the base case, the LWC is highly similar, since LWC is governed by atmospheric dynamics. The median CDNC is smaller by nearly 50% at all heights. The reduction of CDNC is a direct consequence of the absence of ambient CCN. The median values of  $r_m$  are overestimated, consistent with the underestimation of the CDNC.

The simulated total droplet size distributions (i.e. the sum of all the individual distributions considered by the model) at each level are averaged over the total simulation time, taking the conditions mentioned in Sect. 3 into account. In Fig. 4 the averaged size distribution of the simulations with and without the presence of ambient CCN is shown at each observed level. The figure also shows the observed 10%/90% range of droplet concentration as function of radius. This range reflects the variability of LWC and CDNC within the cloud ensemble, associated with e.g. humidity variation and differences in updraft velocity, as will be shown later. The simulated spectra have been interpolated to a resolution consistent with the observations. The spectra simulated in the base case show good agreement with the observed range. The concentration maximum is located at approximately  $8 \mu\text{m}$  radius at 800 m and increases up to  $12 \mu\text{m}$  at 1500 m, agreeing well with the observed peak. The gradual concentration decrease towards smaller droplet radii is consistent with the observed slope, as well as the rapid decrease towards larger radii. In the simulations where the initial specific humidity was varied with 1%, as discussed previously, the slope of the droplet spectra is not altered significantly.

Analysis of the droplet spectra resulting from the simulation without ambient CCN further supports the occurrence of entrainment of fresh CCN. In this simulation, small droplets,  $<5 \mu\text{m}$  radius, are not present, and total droplet concentrations are relatively

## Influence of entrainment of CCN

J. W. B. Derksen et al.

Title Page

Abstract

Introduction

Conclusions

References

Tables

Figures

◀

▶

◀

▶

Back

Close

Full Screen / Esc

Printer-friendly Version

Interactive Discussion



small compared to the observed range. It can be noticed that neglecting entrainment of CCN and the resulting increase of  $r_m$  does not result in a significant increase of precipitable sized droplets for this case. To conclude, comparison of both simulations shows that entrainment of CCN into the cloud at higher altitudes, and subsequent activation to cloud droplets, is an important process in microphysical cloud evolution during RICO.

### 4.3 Role of entrainment and the initial vertical velocity

In Fig. 5, the vertical profiles of the median values of the LWC, CDNC and  $r_m$  are shown for simulations with two different values for the entrainment parameter  $\alpha$ , 0.4 and 0.2, each with an initial vertical velocity,  $w_0$ , of 1.5 m/s and of 1 m/s. The first column corresponds to the base case. The LWC profiles show that an  $\alpha$  of 0.2 leads to an increase of cloud top height with 200 m compared to an  $\alpha$  of 0.4. This is due to less efficient mixing of drier ambient air into the cloud, while a larger part of the released latent heat is used for rising motion and less colder ambient air is entrained. For a smaller value of  $\alpha$  the mixing is reduced. Also the updraft velocities are different, with a maximum value of 2.6 m/s for the simulation with  $\alpha=0.2$ , and 1.8 m/s during the  $\alpha=0.40$  simulation. Although the median of both simulations are similar, the range in simulated LWC for  $\alpha=0.2$  is larger, especially above 1000 m, in better agreement with the observed ranges.

For  $\alpha=0.4$  and  $w_0=1$  m/s, the simulated cloud top altitude is lower than the base case, i.e. 1200 m. Further, the LWC remains smaller and the cloud dissipates earlier through mixing with the environment. Therefore, the cloud top does not reach the levels with enhanced environmental RH, which explains the absence of the secondary peak in LWC below cloud top. If  $\alpha$  is also decreased to 0.2, the cloud top reaches 1700 m. In this case, the simulated and observed median LWC are similar for the lower three observed levels. Just as for the base case and when  $w_0=1.5$  m/s, the model predicts a minimum in the LWC at 1500 m and a maximum just below the cloud top.

For all simulations, the 10% and median values for CDNC are more or less the same

## Influence of entrainment of CCN

J. W. B. Derksen et al.

Title Page

Abstract

Introduction

Conclusions

References

Tables

Figures

◀

▶

◀

▶

Back

Close

Full Screen / Esc

Printer-friendly Version

Interactive Discussion



and agree with the observations. The simulations initialized with  $w_0=1.5$  m/s display a CDNC range up to  $65\text{ cm}^{-3}$ , which is somewhat larger than the simulations initialized with  $w_0=1$  m/s. This reflects the increase of the cutoff radius of activated aerosol with decreasing  $w_0$ .

Decreasing  $\alpha$  does not change the range and median values of  $r_m$ , but the 10% and 90% values are shifted towards larger radii, such that the median values more or less are in the centre. Decreasing  $w_0$  does affect the median and 90% values. Both are slightly smaller,  $0.5\text{--}1\ \mu\text{m}$  at 1000 m altitude. Decreasing both values does not affect the 10% values, but up to 1500 m both median and 90% values have increased with  $0.5\text{--}1\ \mu\text{m}$  and above only the median value has increased with  $0.5\ \mu\text{m}$ , nearly overlapping the observed median values throughout the cloud.

Recapitulating, the entrainment efficiency appears not to influence the median LWC very much, but the occurrence of parcels with relatively high LWC increases. On the other hand, the initial vertical velocity appears to be the dominant influence on the cloud vertical extent and lifetime. It has a large impact on the occurrence of cloud parcels with relatively large LWC, CDNC and cloud drop radius.

Figure 6 shows simulated droplet spectra at 1000 m altitude for each scenario. All three variations display a good agreement with the base case, with concentration maxima at  $10\text{--}11\ \mu\text{m}$ . Largest differences between the droplet spectra are at radii smaller than  $5\ \mu\text{m}$ , which reflects the changes in entrainment with changing values for the parameters  $\alpha$  and  $w_0$ . The different simulations result in droplet peaks at slightly differing radii between  $2\text{--}3\ \mu\text{m}$ , which agrees relatively well with individual observed droplet spectra (not shown). Generally, the simulated distributions are all within the observed variability. Previously it is shown that variations of the entrainment parameter and the initial vertical velocity do not affect profiles of CDNC and droplet radius to a large extent (see Fig. 5), and Fig. 6 shows that the same conclusion is valid for the droplet spectra. This is associated with the nearly constant aerosol concentration vertical profile in the boundary layer during RICO. For such conditions, the changes in droplet concentrations due to detrainment and entrainment appear to balance more or less, and this

## Influence of entrainment of CCN

J. W. B. Derksen et al.

[Title Page](#)[Abstract](#)[Introduction](#)[Conclusions](#)[References](#)[Tables](#)[Figures](#)[◀](#)[▶](#)[◀](#)[▶](#)[Back](#)[Close](#)[Full Screen / Esc](#)[Printer-friendly Version](#)[Interactive Discussion](#)

precludes an accurate assessment of the actual entrainment strength. A larger impact of the entrainment efficiency on CDNC and cloud drop spectra may be expected for steeper aerosol profiles so that the entrained air at higher cloud altitudes has much smaller particle concentrations than air at the cloud base.

5 In summary, the simulations presented here, including those with varying humidity, are well within the observed ranges and reflect, at least partly, the different clouds that make up the RICO ensemble. This supports the idea that this ensemble reflects clouds in different growth stages and growing in varying dynamical conditions associated with spatial variability in atmospheric humidity.

## 10 5 Discussion and conclusions

With a 1-D-cloud column model with detailed calculation of aerosol activation and condensation/evaporation processes, we simulated a trade wind cumulus cloud as observed during RICO (Rain in Cumulus over the Ocean campaign). The simulation reproduces observed profiles of LWC. Simulated CDNC and mean cloud drop radius  
15 agree relatively well with observations. The main discrepancies are an underestimation of LWC below the cloud top, and a slight decrease of CDNC with altitude that is not observed. Discrepancies between model results and observations may partly be explained by spatial humidity variations and by the fact that the observations reflect an ensemble of clouds with different updraft velocities, LWC and vertical extent, whereas  
20 our simulation pertains to a single cloud. It is possible that at higher cloud altitudes the observations are biased towards relatively vigorous cumuli with high updraft velocities and CDNC. This also explains the smaller range of simulated LWC and CDNC, with underestimation of the relative occurrence of higher values.

Turbulent mixing and horizontal variability are not represented by the model. In-  
25 cloud turbulence can lead to redistribution of droplets, resulting in higher local maxima of LWC and CDNC, while  $r_m$  remains the same, although these fluctuations are on the cm scale and should average out at 1 Hz sampling frequency (Pinsky and Khain, 2003;

Title Page

Abstract

Introduction

Conclusions

References

Tables

Figures



Back

Close

Full Screen / Esc

Printer-friendly Version

Interactive Discussion



Grits et al., 2006). However, entrainment of ambient air and subsequent inhomogeneous mixing can lead to in-cloud variations, large enough to sample at 1 Hz (Krueger et al., 1997).

Observed cloud droplet spectra are reproduced well by the model. Simulated and observed maximum concentrations are located at similar droplet radii and simulation shows a gentle slope of the droplet concentration towards smaller radii and a steeper slope towards larger radii, as found in the observations.

We demonstrated that the slope towards small radii is directly associated with the continuous entrainment and subsequent activation of ambient aerosol. The possibility that these droplets are initially present in the cloud column, but activate at higher altitudes under influence of a second saturation peak (Segal et al., 2003) is therefore excluded. Thus, entrainment exerts a significant influence on the droplet size distribution width. It is therefore a crucial factor for the precipitation formation efficiency and optical properties of the cloud. The exchange between cloudy air and environmental air, including the activated and unactivated aerosol particles, must therefore be represented realistically in atmospheric models aimed to study indirect aerosol effects. Further, due to entrainment of aerosol into clouds more particles will be subject to cloud processing (e.g., Roelofs and Kamphuis, 2009) which is relevant for the aerosol direct effect.

When the model is initialized with a smaller initial vertical velocity, all simulated clouds have lower cloud tops and lower LWC maxima. This is consistent with the observations that show that larger vertical velocities are associated with larger LWC.

The entrainment parameter  $\alpha$  influences the dynamical evolution of the simulated cloud, as expressed in LWC and cloud top height. CDNC is only marginally influenced by  $\alpha$ . Particle concentrations inside and outside the cloud are almost equal, so that the in-cloud CCN population is relatively insensitive to the exchange between cloudy and ambient air. It depends on the supersaturation how many of the entrained CCN activate. We found that more subsaturated air is mixed into the cloud when entrainment is more efficient, and this has a negative feedback on the supersaturation. At

## Influence of entrainment of CCN

J. W. B. Derksen et al.

Title Page

Abstract

Introduction

Conclusions

References

Tables

Figures

◀

▶

◀

▶

Back

Close

Full Screen / Esc

Printer-friendly Version

Interactive Discussion



**Influence of  
entrainment of CCN**

J. W. B. Derksen et al.

Title Page

Abstract

Introduction

Conclusions

References

Tables

Figures

◀

▶

◀

▶

Back

Close

Full Screen / Esc

Printer-friendly Version

Interactive Discussion



lower supersaturation values, the cut-off radius is larger and a smaller fraction of the entrained CCN is activated than for less efficient entrainment. A smaller supersaturation also results in less efficient condensation of water vapor and, hence, smaller latent heat release and updraft velocities. Mixing also has a direct negative feedback on the vertical velocity, because the entrained air is at rest and slightly colder than the cloud air. This feeds back on the supersaturation and the entrainment rate. In stratus clouds, spectral broadening of cloud droplets has been associated with variations in updraft velocity at cloud base (Hudson and Yum, 1997). In our study of trade-wind cumuli with lateral entrainment, we find that droplet spectra are relatively insensitive for small variations in  $w_0$  and  $\alpha$ . We conclude that the feedbacks between the vertical motion, supersaturation and the entrainment rate appear to cause a relative balance in cloud growth for the conditions typical of RICO, i.e., a well-mixed boundary layer capped by an inversion.

*Acknowledgements.* Data provided by NCAR/EOL under sponsorship of the National Science Foundation. <http://data.eol.ucar.edu/>

**References**

Albrecht, B. A.: Aerosols, cloud microphysics, and fractional cloudiness, *Science*, 245, 1227–1230, 1989. 8793

Arabas, S., Pawlowska, H., and Grabowski, W. W.: Effective radius and droplet spectral width from in-situ aircraft observations in trade-wind cumuli during RICO, *Geophys. Res. Lett.*, submitted, 2009. 8800

Blyth, A. M. and Latham, J.: Airborne studies of the altitudinal variability of the microphysical structure of small, ice-free, Montanan cumulus clouds, *Q. J. Roy. Meteor. Soc.*, 116, 1405–1423, doi:10.1002/qj.49711649608, 1990. 8794

Burnet, F. and Brenguier, J.-L.: Observational study of the entrainment-mixing process in warm convective clouds, *J. Atmos. Sci.*, 64, 1995–2011, 2007. 8794

Charlson, R. J., Schwarz, S. E., Hales, J. M., Cess, R. D., Jr., J. A. C., Hansen, J. E., and

Hofmann, D. J.: Climate forcing by anthropogenic aerosols, *Science*, 255, 423–430, 1992. 8792

Fountoukis, C. and Nenes, A.: Continued development of a cloud droplet formation parameterization for global climate models, *J. Geophys. Res.*, 110, D11212, doi:10.1029/2004JD005591, 2005. 8793

Gerber, H., Frick, G., Malinowski, S. P., Brenguier, J.-L., and Burnet, F.: Holes and entrainment in stratocumulus, *J. Atmos. Sci.*, 62, 443–459, 2005. 8793

Gerber, H., Frick, G., Jensen, J. B., and Hudson, J. G.: Entrainment, mixing and microphysics in trade-wind cumulus, *J. Meteorol. Soc. Jpn.*, 86A, 87–106, 2008. 8795, 8797, 8798

Grits, B., Pinsky, M., and Khain, A.: Investigation of small-scale droplet concentration inhomogeneities in a turbulent flow, *Meteor. Atmos. Phys.*, 92, 191–204, doi:10.1007/s00703-005-0157-4, 2006. 8805

Hänel, G.: The role of aerosol properties during the condensational stage of cloud: A reinvestigation of numerics and microphysics, *Beitr. Phys. Atmosph.*, 60, 321–339, 1987. 8793, 8796

Hicks, E., Pontikis, C., and Rigaud, A.: Entrainment and mixing processes as related to droplet growth in warm midlatitude and tropical clouds, *J. Atmos. Sci.*, 47, 1589–1618, 1990. 8794

Hudson, J. G. and Mishra, S.: Relationship between CCN and cloud microphysics variations in clean maritime air, *Geophys. Res. Lett.*, 34, L16804, doi:10.1029/2007GL030044, 2007. 8798

Hudson, J. G. and Yum, S. S.: Droplet spectral broadening in Marine Stratus, *J. Atmos. Sci.*, 54, 2642–2654, 1997. 8806

Jacobson, M. Z.: *Fundamentals of Atmospheric Modeling*, Cambridge Univ. Press, New York, 1998. 8796

Kreidenweis, S., Walcek, C., Feingold, G., Gong, W., Jacobson, M., Kim, C., Liu, X., Penner, J., Nenes, A., and Seinfeld, J.: Modification of aerosol mass and size distribution due to aqueous phase SO<sub>2</sub> oxidation in clouds: Comparisons of several models, *J. Geophys. Res.*, 108, 4213, doi:10.1029/2002JD002697, 2003. 8794

Krueger, S. K., Su, C.-W., and McMurtry, P. A.: Modeling entrainment and finescale mixing in cumulus clouds, *J. Atmos. Sci.*, 54, 2697–2712, 1997. 8805

Kulmala, M., Laaksonen, A., Korhonen, P., Ahonen, T., and Baret, J.: The effect of atmospheric nitric acid vapor on cloud condensation nucleus activation, *J. Geophys. Res.*, 98, 22949–22958, 1993. 8793

**Influence of entrainment of CCN**

J. W. B. Derksen et al.

Title Page

Abstract

Introduction

Conclusions

References

Tables

Figures

◀

▶

◀

▶

Back

Close

Full Screen / Esc

Printer-friendly Version

Interactive Discussion



- Lohmann, U. and Feichter, J.: Global indirect aerosol effects: a review, *Atmos. Chem. Phys.*, 5, 715–737, 2005,  
<http://www.atmos-chem-phys.net/5/715/2005/>. 8793
- Lu, M.-L., Wang, J., Freedman, A., Jonsson, H. H., Flagan, R. C., McClatchey, R. A., and Seinfeld, J. H.: Analysis of humidity halos around trade wind cumulus clouds, *J. Atmos. Sci.*, 60, 1041–1059, 2003. 8799
- Meskhidze, N., Nenes, A., Conant, W. C., and Seinfeld, J. H.: Evolution of a new cloud droplet activation parameterization with in situ data from CRYSTAL-FACE and CSTRIFE, *J. Geophys. Res.*, 110, D16202, doi:10.1029/2004JD005703, 2005. 8793
- Ogura, Y. and Takahashi, T.: Numerical simulation of the life cycle of a thunderstorm cell, *Mon. Weather Rev.*, 99, 895–911, 1971. 8795
- Paluch, I. R.: Mixing and the cloud droplet size spectrum: Generalizations from the CCOPE data, *J. Atmos. Sci.*, 43, 1984–1993, 1986. 8794
- Penner, J. E. and Chuang, C. C.: The role of entrainment and mixing in altering the relationship between aerosol concentration and cloud drop number concentration, Ninth ARM Science Team Meeting Proceedings, 1999. 8793
- Peter, J. R., Blyth, A. M., Brooks, B., McQuaid, J. B., Lingard, J. J. N., and Smith, M. H.: On the composition of Caribbean maritime aerosol particles measured during RICO, *Q. J. Roy. Meteor. Soc.*, 134, 1059–1063, doi:10.1002/qj.198, 2008. 8799
- Pinsky, M. and Khain, A.: Fine structure of cloud droplet concentrations as seen from the fast-FSSP measurements. Part II: Results of in situ observations, *J. Appl. Meteorol.*, 42(1), 65–73, 2003. 8804
- Pruppacher, H. R. and Klett, J. D.: *Microphysics of clouds and precipitation*, D. Reidel, Dordrecht, 1978. 8793, 8794
- Rauber, R., Stevens, B., Ochs, H., Knight, C., Albrecht, B., Blyth, A., Fairall, C., Jensen, J., Lasher-Trapp, S., Mayol-Bracero, O., Vali, G., Anderson, J., Baker, B., Bandy, A., Burnet, E., Brenguier, J., Brewer, W., Brown, P., Chuang, P., Cotton, W., Girolamo, L. D., Geerts, B., Gerber, H., Gke, S., Gomes, L., Heikes, B., Hudson, J., Kollias, P., Lawson, R., Krueger, S., Lenschow, D., Nuijens, L., O’Sullivan, D., Rilling, R., Rogers, D., Siebesma, A., Snodgrass, E., Stith, J., Thornton, D., Tucker, S., Twohy, C., and Zuidema, P.: Rain In Shallow Cumulus over the Ocean: The RICO Campaign, *B. Am. Meteorol. Soc.*, 88, 1912–1928, 2007. 8794
- Roelofs, G.-J. and Jongen, S.: A model study of the influence of aerosol size and chemical properties on precipitation formation in warm clouds, *J. Geophys. Res.*, 109, D22201,

**Influence of  
entrainment of CCN**

J. W. B. Derksen et al.

Title Page

Abstract

Introduction

Conclusions

References

Tables

Figures

◀

▶

◀

▶

Back

Close

Full Screen / Esc

Printer-friendly Version

Interactive Discussion



doi:10.1029/2004JD004779, 2004. 8793, 8794, 8795

Roelofs, G.-J. and Kamphuis, V.: Cloud processing, cloud evaporation and Angström exponent, Atmos. Chem. Phys., 9, 71–80, 2009,

<http://www.atmos-chem-phys.net/9/71/2009/>. 8793, 8805

5 Roesner, S., Flossmann, A. I., and Pruppacher, H. R.: The effect on the evolution of the drop spectrum in clouds of the preconditioning of air by successive convective elements, Q. J. Roy. Meteor. Soc., 116, 1389–1403, doi:10.1002/qj.49711649607, 1990. 8794

Segal, Y., Pinsky, M., Khain, A., and Erlick, C.: Thermodynamic factors influencing bimodal spectrum formation in cumulus clouds, Atmos. Res., 66, 43–64, 2003. 8805

10 Solomon, S., Qin, D., Manning, M., Alley, R. B., Berntsen, T., Bindoff, N. L., Chen, Z., Chidthaisong, A., Gregory, J. M., Hegerl, G. C., Heimann, H., Hewitson, B., Hoskins, B. J., Joos, F., Jouzel, J., Kattsov, V., Lohmann, U., Matsuno, T., Molina, M., Nichollsand, N., Overpeck, J., Raga, G., Ramaswamy, V., Ren, J., Rusticucci, M., Somerville, R., Stocker, T. F., Whetton, P. A. W. R., and Wratt, D.: Technical Summary, in: Climate Change 2007: The Physical Science Basis. Contribution of Working Group I to the Fourth Assessment Report of the Intergovernmental Panel on Climate Change, Cambridge Univ. Press, Cambridge, United Kingdom and New York, NY, USA, 2007. 8792

15 Su, C.-W., Krueger, S. K., McMurtry, P. A., and Austin, P. H.: Linear eddy modeling of droplet spectral evolution during entrainment and mixing in cumulus clouds, Atmos. Res., 47-48, 41–58, 1998. 8793, 8794

20 Takahashi, T.: Warm rain, giant nuclei and chemical balance -a numerical model, J. Atmos. Sci., 33, 269–286, 1976. 8795

Twomey, S.: The influence of pollution on the shortwave albedo of clouds, J. Atmos. Sci., 34, 1149–1154, 1977. 8792

ACPD

9, 8791–8816, 2009

---

## Influence of entrainment of CCN

J. W. B. Derksen et al.

---

Title Page

Abstract

Introduction

Conclusions

References

Tables

Figures

◀

▶

◀

▶

Back

Close

Full Screen / Esc

Printer-friendly Version

Interactive Discussion



**Influence of  
entrainment of CCN**

J. W. B. Derksen et al.

**Table 1.** Parameters for the aerosol size distribution: aerosol concentration ( $n$ ,  $\text{cm}^{-3}$ ), mean aerosol radius ( $r_m$ ,  $\mu\text{m}$ ) and standard deviation ( $\sigma$ ).

Mode	$n$ ( $\text{cm}^{-3}$ )	$r_m$ ( $\mu\text{m}$ )	$\sigma$
1	118	0.019	3.3
2	11	0.056	1.6
3	0.1	0.8	2.2

[Title Page](#)[Abstract](#)[Introduction](#)[Conclusions](#)[References](#)[Tables](#)[Figures](#)[I◀](#)[▶I](#)[◀](#)[▶](#)[Back](#)[Close](#)[Full Screen / Esc](#)[Printer-friendly Version](#)[Interactive Discussion](#)

**Influence of  
entrainment of CCN**

J. W. B. Derksen et al.

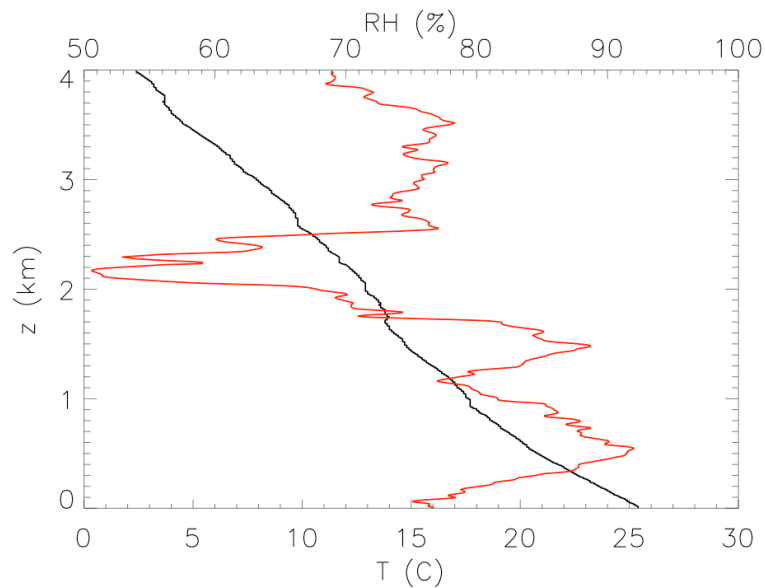


**Fig. 1.** Vertical profiles of temperature (black) and relative humidity (red), from drop sonde.

[Title Page](#)[Abstract](#)[Introduction](#)[Conclusions](#)[References](#)[Tables](#)[Figures](#)[◀](#)[▶](#)[◀](#)[▶](#)[Back](#)[Close](#)[Full Screen / Esc](#)[Printer-friendly Version](#)[Interactive Discussion](#)

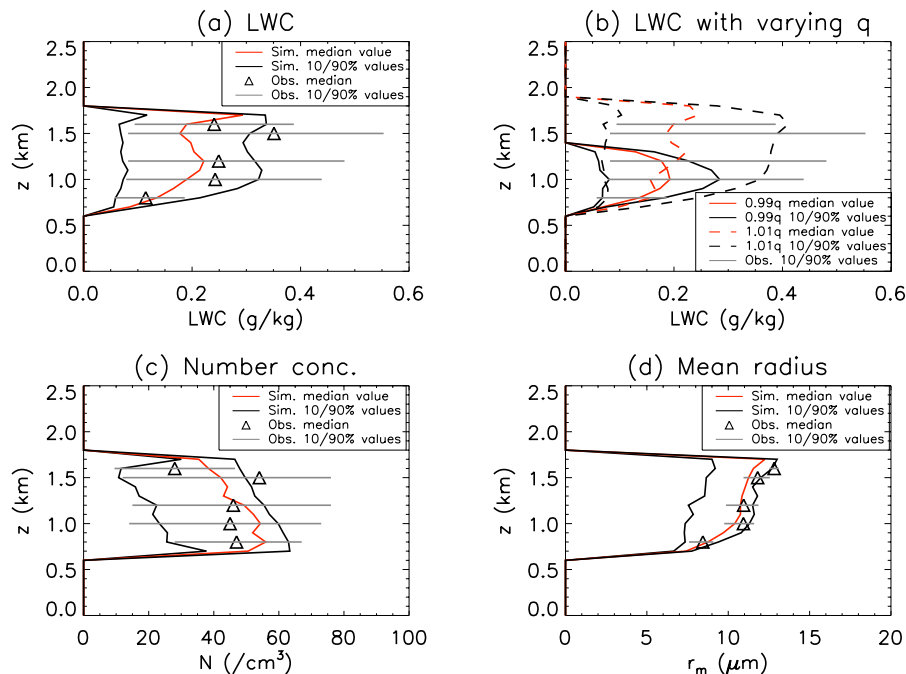


**Fig. 2.** Vertical profiles of the simulated (red) and observed (triangles) median values of **(a)** LWC, **(c)** droplet number concentration and **(d)**  $r_m$  of the base case. **(b)** shows vertical profiles of the median values of the LWC of the simulations with 99% and 101% of the specific humidity (respectively red solid and broken lines). Simulated 10 and 90% values are depicted with solid (broken) black lines. The horizontal grey lines through the triangles depict the observed range between the 10% and the 90% values.

[Title Page](#)
[Abstract](#)
[Introduction](#)
[Conclusions](#)
[References](#)
[Tables](#)
[Figures](#)
[◀](#)
[▶](#)
[◀](#)
[▶](#)
[Back](#)
[Close](#)
[Full Screen / Esc](#)
[Printer-friendly Version](#)
[Interactive Discussion](#)


Influence of  
entrainment of CCN

J. W. B. Derksen et al.

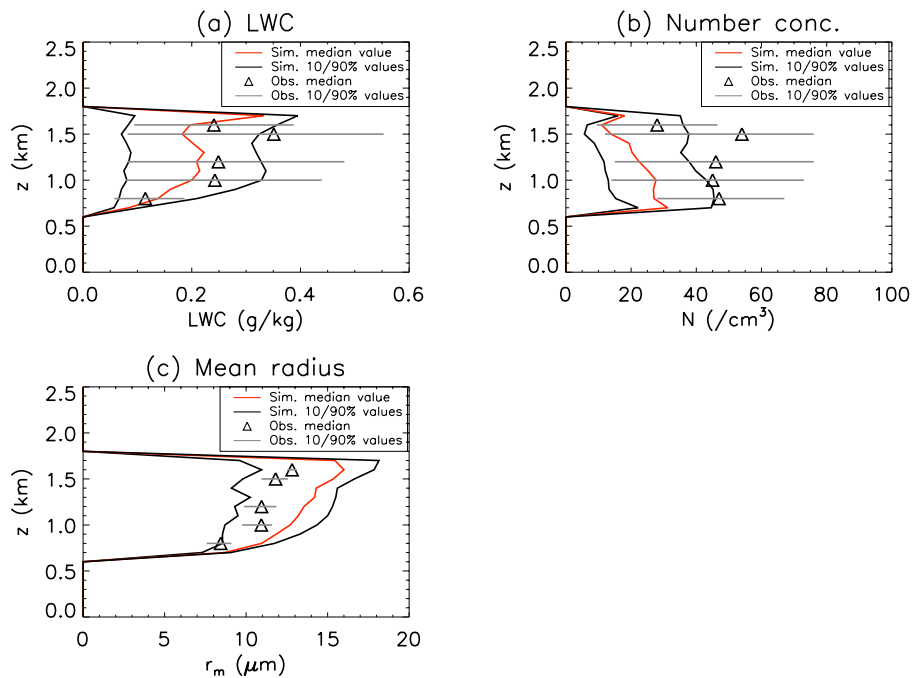


**Fig. 3.** As Fig. 2, but for the simulation without the presence of ambient CCN.

[Title Page](#)[Abstract](#)[Introduction](#)[Conclusions](#)[References](#)[Tables](#)[Figures](#)[I◀](#)[▶I](#)[◀](#)[▶](#)[Back](#)[Close](#)[Full Screen / Esc](#)[Printer-friendly Version](#)[Interactive Discussion](#)

Influence of  
entrainment of CCN

J. W. B. Derksen et al.

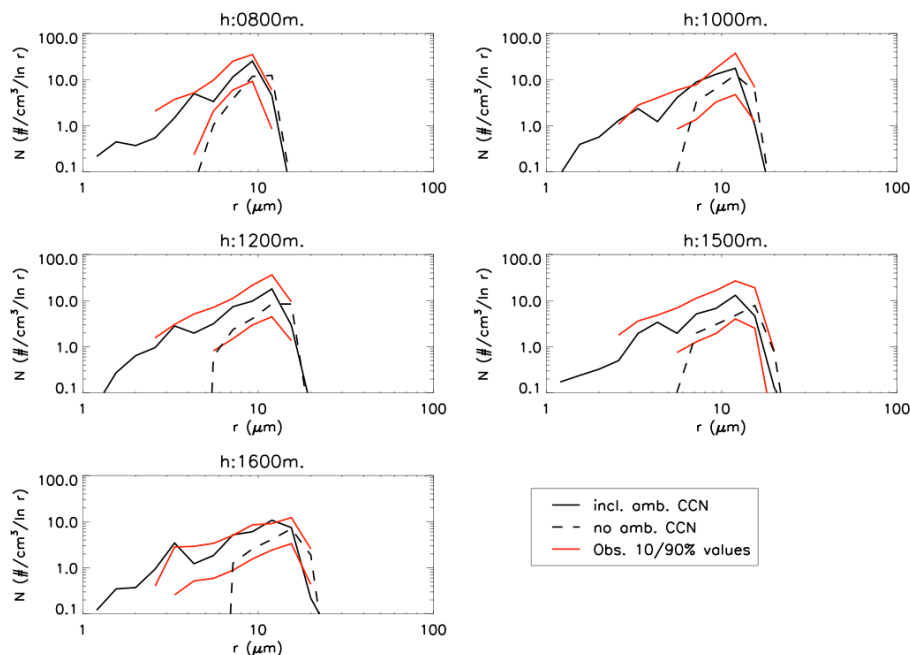


**Fig. 4.** Time averaged cloud droplet size distributions for: 800, 1000, 1200, 1500 and 1600 m altitude from the simulation with (solid) and without (broken) entrainment of ambient CCN. Red lines reflect the observed 10 and 90% values.

[Title Page](#)[Abstract](#)[Introduction](#)[Conclusions](#)[References](#)[Tables](#)[Figures](#)[◀](#)[▶](#)[◀](#)[▶](#)[Back](#)[Close](#)[Full Screen / Esc](#)[Printer-friendly Version](#)[Interactive Discussion](#)

Influence of  
entrainment of CCN

J. W. B. Derksen et al.

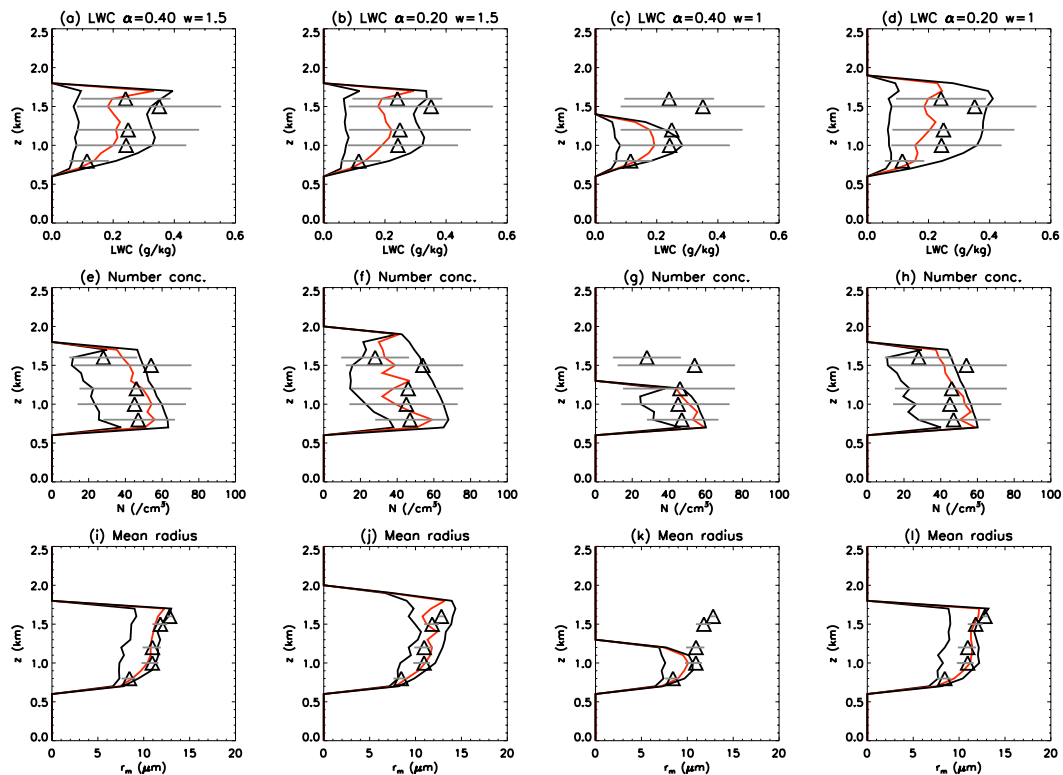


**Fig. 5.** As Fig. 2, but for four simulations: First column: base case,  $\alpha=0.4$ ,  $w_0=1.5$  m/s; second column:  $\alpha=0.2$ ,  $w_0=1.5$  m/s; third column  $\alpha=0.4$ ,  $w_0=1$  m/s; fourth column:  $\alpha=0.2$ ,  $w_0=1$  m/s.

Title Page

Abstract

Introduction

Conclusions

References

Tables

Figures

◀

▶

◀

▶

Back

Close

Full Screen / Esc

Printer-friendly Version

Interactive Discussion



Influence of  
entrainment of CCN

J. W. B. Derksen et al.

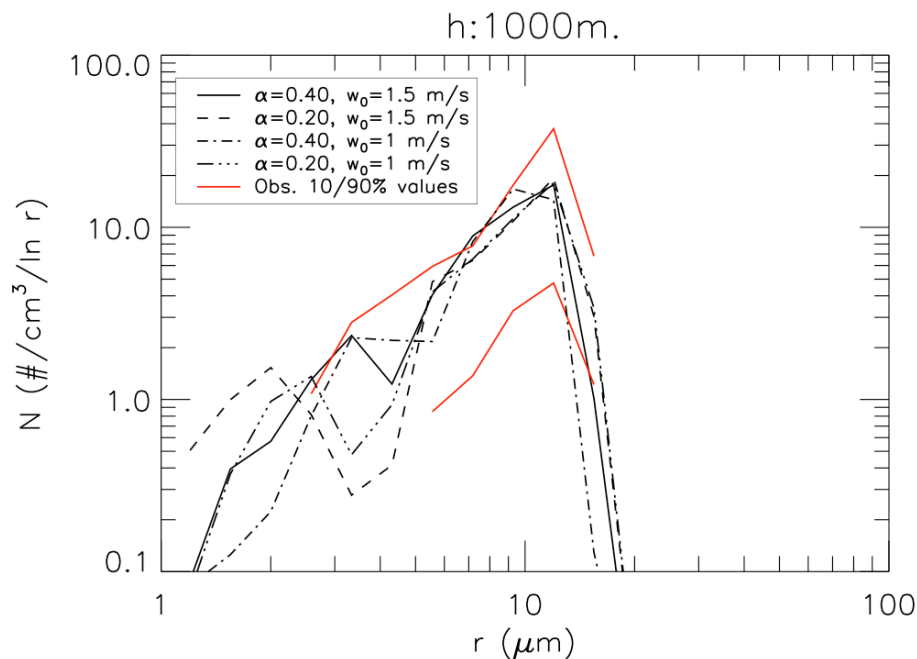


**Fig. 6.** Time averaged cloud droplet size distributions at 1000 m height for four simulations: base case (solid black line),  $\alpha=0.2$  and  $w_0=1.5$  m/s (dashed line),  $\alpha=0.4$  and  $w_0=1$  m/s (dot-dashed line) and  $\alpha=0.2$  and  $w_0=1$  m/s (dot-dot-dashed-line). In red are the 10 and 90% values from the observations.

[Title Page](#)[Abstract](#)[Introduction](#)[Conclusions](#)[References](#)[Tables](#)[Figures](#)[◀](#)[▶](#)[◀](#)[▶](#)[Back](#)[Close](#)[Full Screen / Esc](#)[Printer-friendly Version](#)[Interactive Discussion](#)